Rates of deposition, uplift and erosion in the Swiss Molasse basin, estimated from sonic - and density - logs

Rates of Deposition, Uplift and Erosion in the Swiss Molasse Basin, Estimated from Sonic - and Density - Logs

by

B. Kaelin[1,2], L. Rybach[1] and E.H.K. Kempter[3]

Abstract

Deposition/subsidence and uplift/erosion are key processes in the development of sedimentary basins. For paleogeothermal reconstructions the estimation of the total burial depth (including sections now eroded) is needed. The amount of erosional discordance can be inferred from compaction, which in turn can be estimated from borehole data, by extrapolation from sonic and density logs.

Sonic and density logs from different localities in the Swiss Molasse basin were evaluated to yield porosity-depth profiles. From these, compaction parameters for different lithologies like sandstones, shales and limestones were determined, assuming exponential decrease of porosity with depth. The results were then used to calculate subsidence/uplift diagrams for the localities studied, by taking the effect of compaction into account.

According to compaction trends, late to post-Tertiary erosional gaps in the central Swiss Molasse basin range from about 4 km at Schafisheim in the north to as much as 8.5 km for the overthrusted Molasse at Thun-1 in the south — much larger than expected from previous views based on regional geology. The sediments were deposited at rates of 0.1 to 0.6 mm/a.

According to subsidence/uplift diagrams of different sites, the sediments of the northern and southern parts of the Molasse basin compacted differently: The southern part is characterized by at least two separate major subsidence phases. The younger one is presumably caused by overthrusting of the Subalpine Molasse unit. The influence of lateral tectonic stress on compaction still needs to be investigated. The same holds true for effects of early cementation, overpressure and secondary porosity due to corrosive subsurface fluids.

Introduction

Attempts to delineate oil and gas prospective areas require an understanding of the evolution of the sedimentary basin in question. Deposition/subsidence and uplift/erosion are key processes in basin development. For paleogeothermal reconstruction, especially in the context of using maturity trends of organic matter, the estimation of total burial depth (including sections now eroded) is needed. The amount of erosional discordance can be inferred from compaction trends, which in turn can be estimated from sonic and density logs. The key to this approach is the observed general dependence of porosity on burial depth. It is customary to approximate the decrease of porosity with depth by an exponential function (see e.g. MAGARA, 1978).

In a first attempt to estimate possible patterns of uplift/erosion and of erosional gaps, the following procedure was applied: Sonic and density logs from different boreholes in the Swiss Molasse basin were processed by standard techniques to yield porosity-depth profiles, ignoring possible effects of lateral stress and/or anomalous pore pressures on compaction at this stage. From these profiles, compaction parameters were determined for different lithologies, such as sandstones, shales and limestones. The re-

1) Institute of Geophysics ETHZ, CH-8093 Zurich, Switzerland

2) now at POLYDYNAMICS Ltd., CH-8032 Zurich, Switzerland

3) RICO RESEARCH, CH-5443 Niederrohrdorf, Switzerland

sults were then used to construct subsidence/uplift diagrams for the localities studied, by taking into account the effect of compaction. From the diagrams, the timing of subsidence/uplift events can be estimated as well as the rates of uplift and erosion.

The purpose of this paper is to outline an approach for the reconstruction of compaction trends and for the construction of compaction-corrected burial history diagrams, using selected examples from the Swiss sector of the Molasse Basin.

Determination of Porosity/Depth Trends

The starting base (lithologic-stratigraphic profiles, sonic (BHC) and density (LDT) logs) was taken for the drillholes Weiach and Schafisheim, which are part of a radioactive waste disposal reconnaissance study, from WEBER et al. (1986), and for the gas exploration drillhole Thun-1. The data of SWISSPETROL AG were accessible through the «Bundesamt fuer Energiewirtschaft».

The approach used in this study is outlined in Figure 1 which shows the different steps of the procedure applied. Maximum burial depth can be estimated from sonic travel time-depth profiles or from porosity-depth profiles.

The object of the present study is the Swiss Molasse basin in the northern Foreland of the Alps. Figure 2 shows the western end of the Molasse basin. The dotted areas represent the Tertiary formation of the Molasse Basin and the Rhine Graben (after HOMEWOOD et al., 1986). The sites of the investigated drillholes are indicated by solid dots.
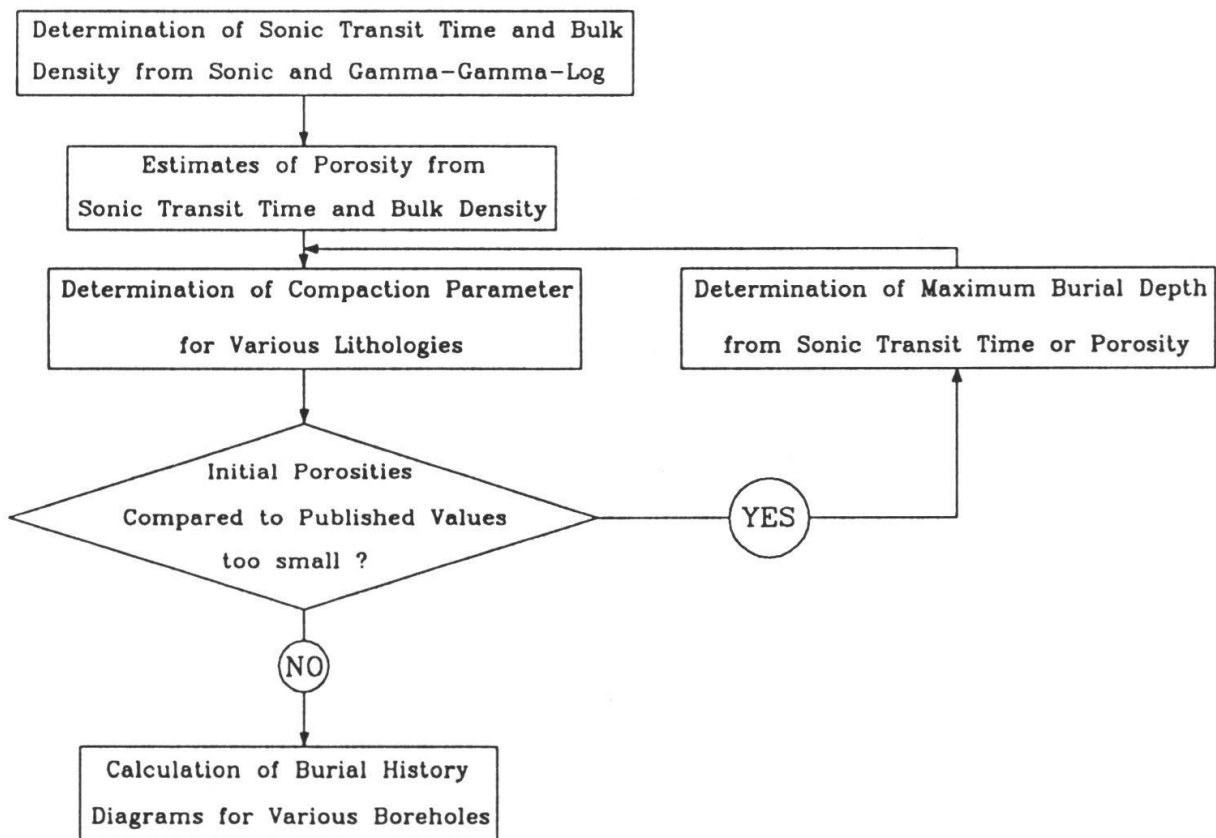

Figure 1 Different steps of the approach to determine maximum burial depth and burial history.
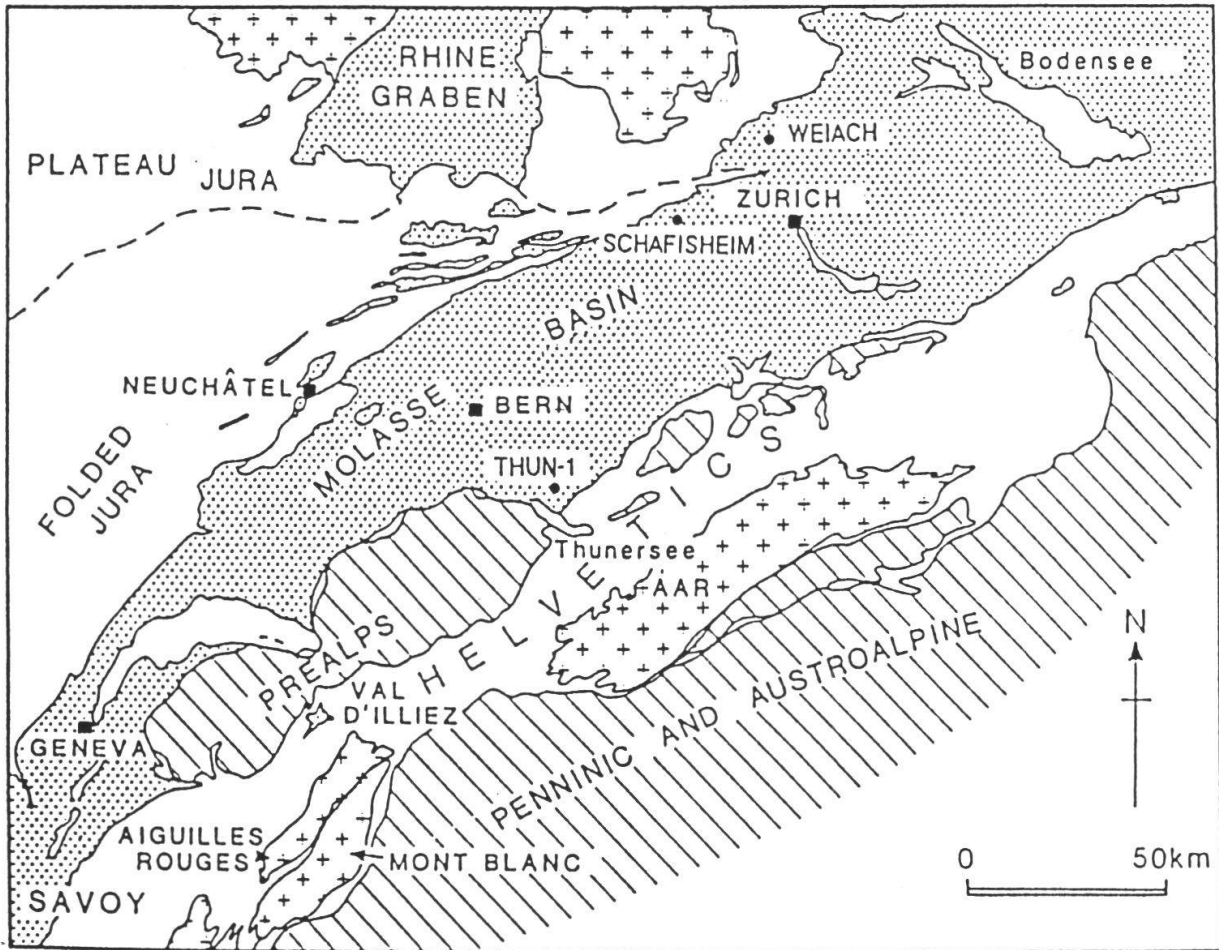
10

Figure 2 The Swiss Molasse basin and its geological framework, with the location of the investigated drillholes Weiach, Schafisheim and Thun-1.

Standard procedures were applied to determine porosity from density (gamma-gamma) and sonic logs. The following equations were used:

$$\Phi = (\rho_m - \rho_{log}) / (\rho_m - \rho_f) \qquad (1)$$

for processing the density log. Here is Φ (in decimals) the rock porosity, ρ_m the matrix density, ρ_{log} the bulk density as measured by the log, and ρ_f the density of the pore fluid. Further for the sonic log

$$\Phi = (\Delta t_{log} - \Delta t_m) / (\Delta t_f - \Delta t_m) \qquad (2)$$

where Δt_{log} is the sonic travel time measured by the log (in $\mu s/m$), Δt_m the sonic travel time in the rock matrix, and Δt_f the sonic travel time in the pore fluid. These equations contain reference values of sonic travel time and density for rock matrix and pore fluid (Δt_m, Δt_f; ρ_m, ρ_f); these values (for different lithologies) were taken from DRESSER ATLAS (1982).

Since two independent indications of porosity are available at any given depth (one from the sonic and another from the density log), the correlation method of HEGARTY et al. (1988) can be used to estimate average porosity. This method works with a best fit of the bulk density/sonic travel time function and with the correlation (1:1 in the ideal case) between the porosities determined from sonic and density logs The method yields the average porosity at the depth in question.

11

Figure 3 shows the porosity/depth-dependence at the Weiach drillsite in six lithologies. The same six lithologies were distinguished throughout this study. The figure also shows the stratigraphic column of the Weiach drillhole. The sequence contains at least seven unconformities of different magnitude, with 3-4 of them representing major erosional gaps.
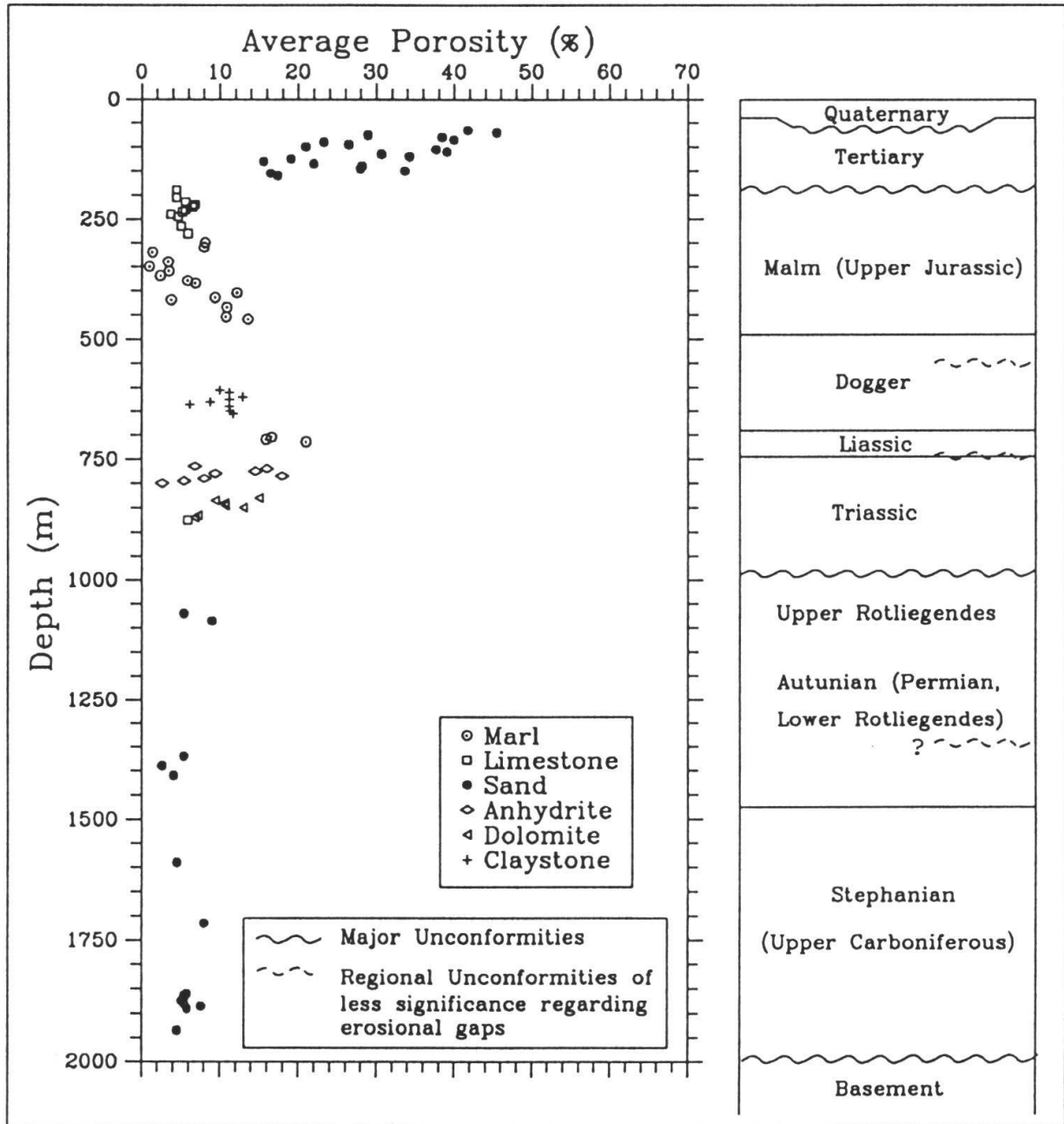

Figure 3 Stratigraphic column and porosity/depth dependence at the Weiach drillsite. These six lithologies distinguished are used througout the whole study.

It is customary to approximate porosity/depth data sets by an exponential law (MAGA-RA, 1978):

$$\Phi(z) = \Phi_0 \exp(-z/CK) \tag{3}$$

12

where z is the depth (in m), $\Phi(z)$ the porosity as a function of the depth, Φ_0 the initial porosity (i.e. the porosity at $z = 0$), and CK the characteristic depth (m). Equation (3) gives porosity as a function of burial depth and contains two specific parameters: The surface porosity Φ_0 and the characteristic depth CK. Both parameters depend on lithology.

Determination of Compaction Parameters for Different Lithologies

The parameters Φ_0 and CK are indicative of compactional trends. They have been determined for six different lithologies, from the three investigated boreholes in the Swiss Molasse basin. Figure 4 shows the porosity/depth data set for autochthonous Tertiary sandstones; TABLE 1 shows the compaction parameters Φ_0 and CK found for the six lithologies. The compaction parameters were determined by best fit lines.
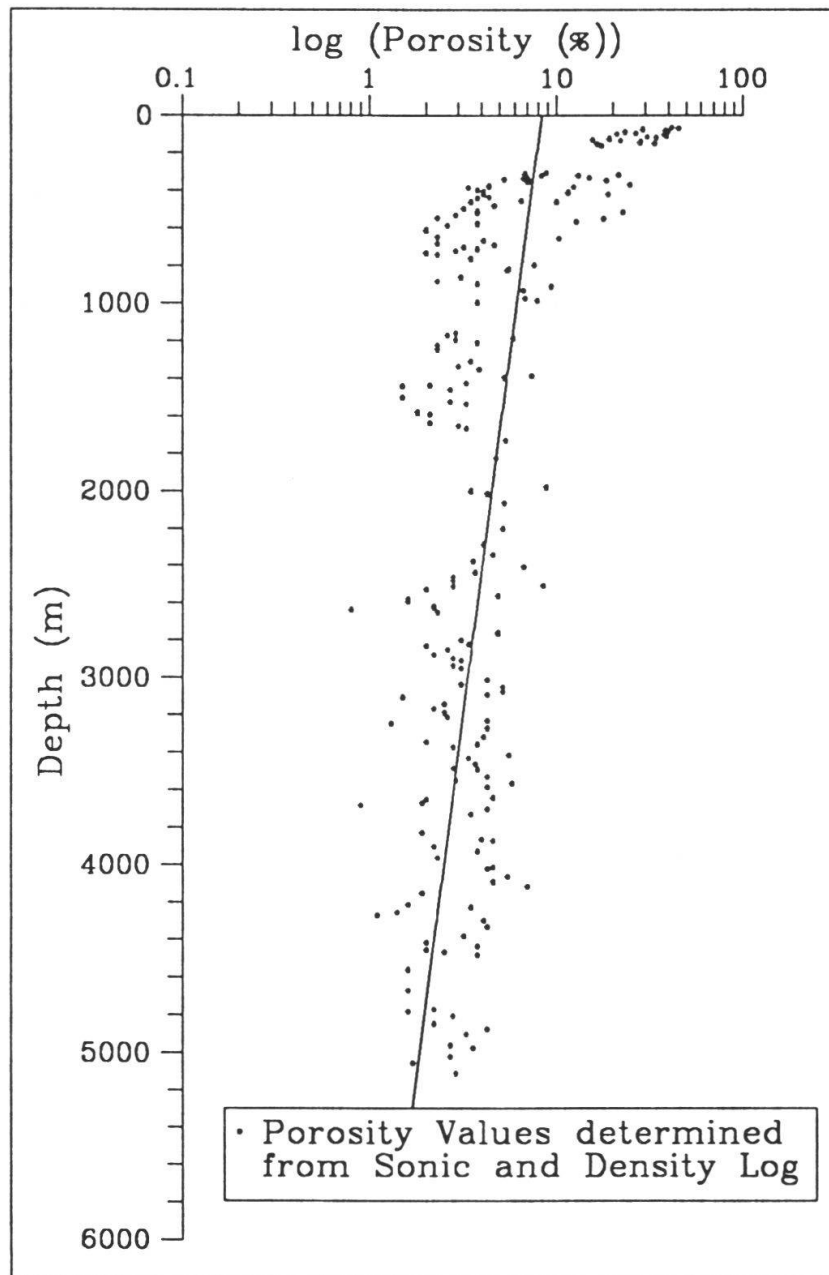

Figure 4 Porosity/depth dependence for a particular lithology: Autochthonous Tertiary sandstones.

13

Table 1 Compaction Parameters Φ_0 and CK for Different Lithologies

Lithology	Φ_0	CK (m)
Marl	7 ± 1	6560 ± 1610
Limestone	5 ± 1	14400 ± 2570
Sand	17 ± 2	2080 ± 80
Anhydrite	16 ± 10	1390 ± 1200
Dolomite	48 ± 48	580 ± 220
Claystone/Shale	8 ± 1	7030 ± 1550

Determination of Maximum Burial Depth/Amount of Erosion

Table 1 shows Φ_0 values for the lithologies marl, limestone and shale which are — in comparison to published values — much too low. Also, the «surface» porosity for sandstones is much lower than the value of 40% which should be expected (HOUSE-KNECHT, 1987). Therefore it must be concluded that the rocks investigated in this study were at greater burial depths at one time in their geologic past than they are at present; their relatively low porosity must be the result of considerable extra burial. Or else, other factors, not accounted for at the present stage, must have contributed to this exceedingly low porosity, such as lateral tectonic stress or diagenetic effects, related to anomalous pore pressures.

The difference between present-day depth and maximum depth of burial was determined by the following procedure: The porosity/depth profiles were plotted on a logarithmic scale and shifted along the z axis to minimize the difference between measured and reference profiles (for the same lithology). The difference $\Delta(z)$ between measured and theoretically expected depth is defined by equ. (4):

$$\Delta(z) = (1/n) \sum_{i=1}^{n} (\ln \Phi_{me}(z_0 + \Delta z_i) - \ln \Phi_{th}(z + \Delta z_i))^2 \qquad (4)$$

where $\Delta(z)$ is the difference in function of depth z (m), n the number of porosity values measured for a particular lithology, z the variable depth in that particular lithology, z_0 the depth (m) from surface for the particular lithology, Δz_i the difference between the depth of the measured Φ value and the z_0, $\Phi_{me}(Z_0 + \Delta z_i)$ porosity measured at the depth $(z_0 + \Delta z_i)$, and $\Phi_{th}(z + \Delta z_i)$ the theoretical porosity at the depth $(z + \Delta z_i)$, according to a particular porosity-depth function.

The depth differences (maximum depth minus present depth) by minimizing $\Delta(z)$ found are shown on Figure 5. The compilation of the maximum amounts of erosion as calculated is given in Table 2.

Having determined the erosional gaps for each borehole, the parameters Φ_0 and CK can be calculated for the different lithologies. The Φ_0 values correspond now to the values reported in the literature (HEGARTY et al., 1988; ISSLER & BEAUMONT, 1989; SCLATER & CHRISTIE, 1980; SCHMOCKER & HALLEY, 1982; SCHOLLE & HALLEY, 1983). More details are given in KAELIN (1990).
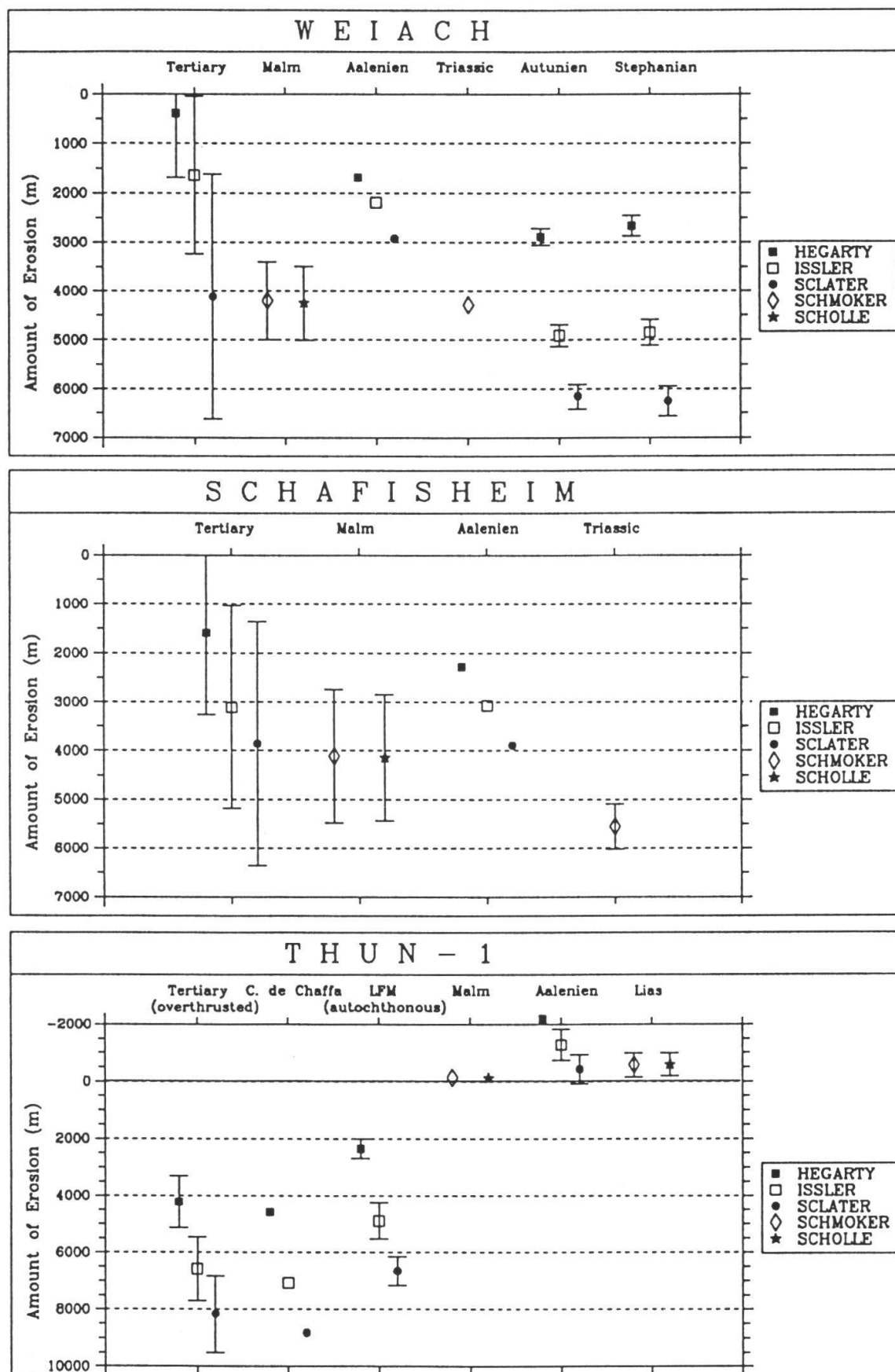
14

Figure 5 The maximum amount of erosion, as calculated by using lithologydependent parameters, published by HEGARTY et al. (1988), ISSLER & BEAUMONT (1989), SCLATER & CHRISTIE (1980), SCHMOCKER & HALLEY (1982), SCHOLLE & HALLEY (1983).

Table 2 Tertiary Erosional Gaps, Derived from Porosity/Depth Profiles

Borehole	Stratigraphic Unit	Maximum Amount of Erosion (m)		
Weiach	Tertiary, Mesozoic & Permocarboniferous	3885	±	660
Schafisheim	Tertiary & Mesozoic	4355	±	385
Thun-1	Tertiary, overthrusted	8490	±	680
	Tertiary, autochthonous	6650	±	500
	Mesozoic	-370	±	230

Subsidence Curves, Taking into Account the Effect of Compaction

Subsidence curves show the burial history of sedimentary formations as they move to their present depth through time. The effect of compaction can significantly influence the subsidence rate (see Figure 6). The effect of compaction can be considered by taking into account the thickness decrease of a given sedimentary interval during successive stages of burial. For example, a sedimentary layer with an original thickness of 1600 m near the surface is reduced to 1000 m thickness at depth (now between -5 and -6 km).
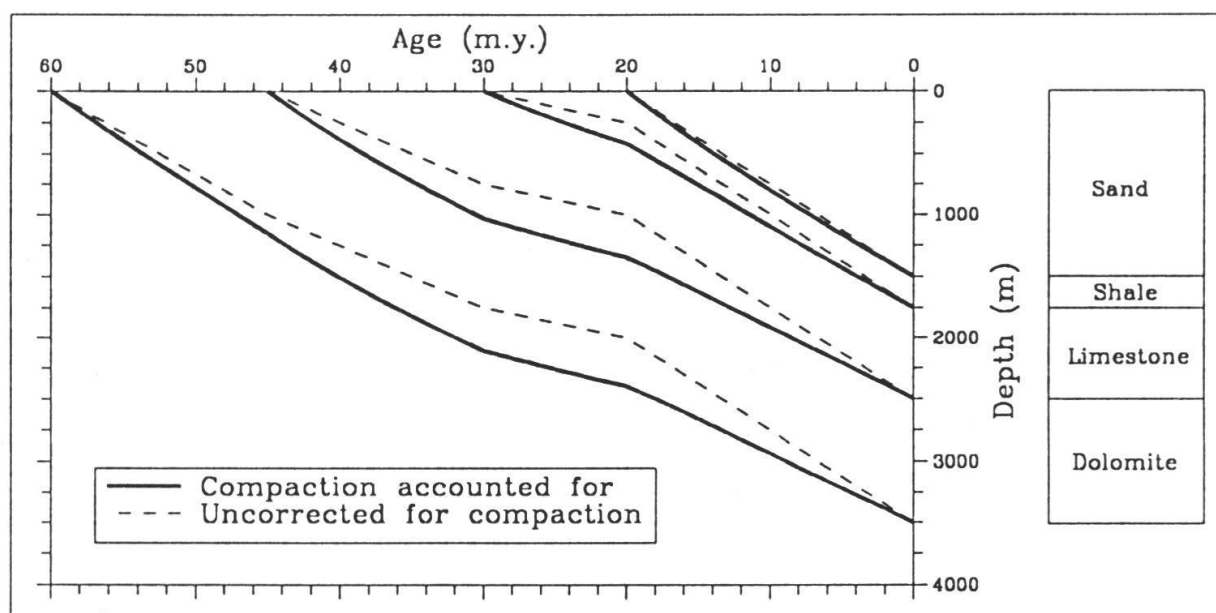
Figure 6 Burial history curves with and without correction for compaction (schematic).

The problem in calculating the effect of compaction is to determine the correct depth of the base of a particular sedimentary interval. The following procedure was used: It can be assumed, that the amount of solid material (represented by the solid height h_s) remains constant during burial; i.e. only the pore volume decreases. Equ.(5) relates h_s to the porosity/depth function $\Phi(z)$, according to the classical paper of PERRIER & QUIBLIER (1974):

16

$$h_s = \int_{z_1}^{z_2} (1 - \Phi(z))dz \qquad (5)$$

where h_s is solid height (m), z_1 the depth to the top and z_2 to the bottom of a particular layer (m), and $\Phi(z)$ the porosity (as decimals) as a function of depth z.

In the approach outlined in this paper an exponential porosity/depth function according to equ.(3) was used. Inserting equ.(3) to equ.(5) yields, after integration, equ.(6):

$$h_s = (z_2 - z_1) + \Phi_0 \, CK \, [exp(-z_2/CK) - exp(-z_1/CK)] \qquad (6)$$

This non-linear equation cannot be solved analytically to yield the unknown z_2. After some rewriting, equ.(7) results:

$$f(x) = x + \Phi_0 \, exp(-x) - k = 0 \qquad (7)$$

with
$$k = x + \Phi_0 \, exp(-x)$$
$$k = (h_s/CK) + (z_1/CK) + \Phi_0 \, exp(-z_1/CK)$$
$$x = z_2/CK.$$

Equ.(7) can be solved by numerical iteration (finding the root, i.e. the value of x at which $f(x) = 0$). The *regula falsi* method was applied for this purpose.

After having determined z_2 for a given layer, the procedure is repeated for the neyt deeper layer (the top of which is at z_2). The process is repeated until the base of the sediments is reached.
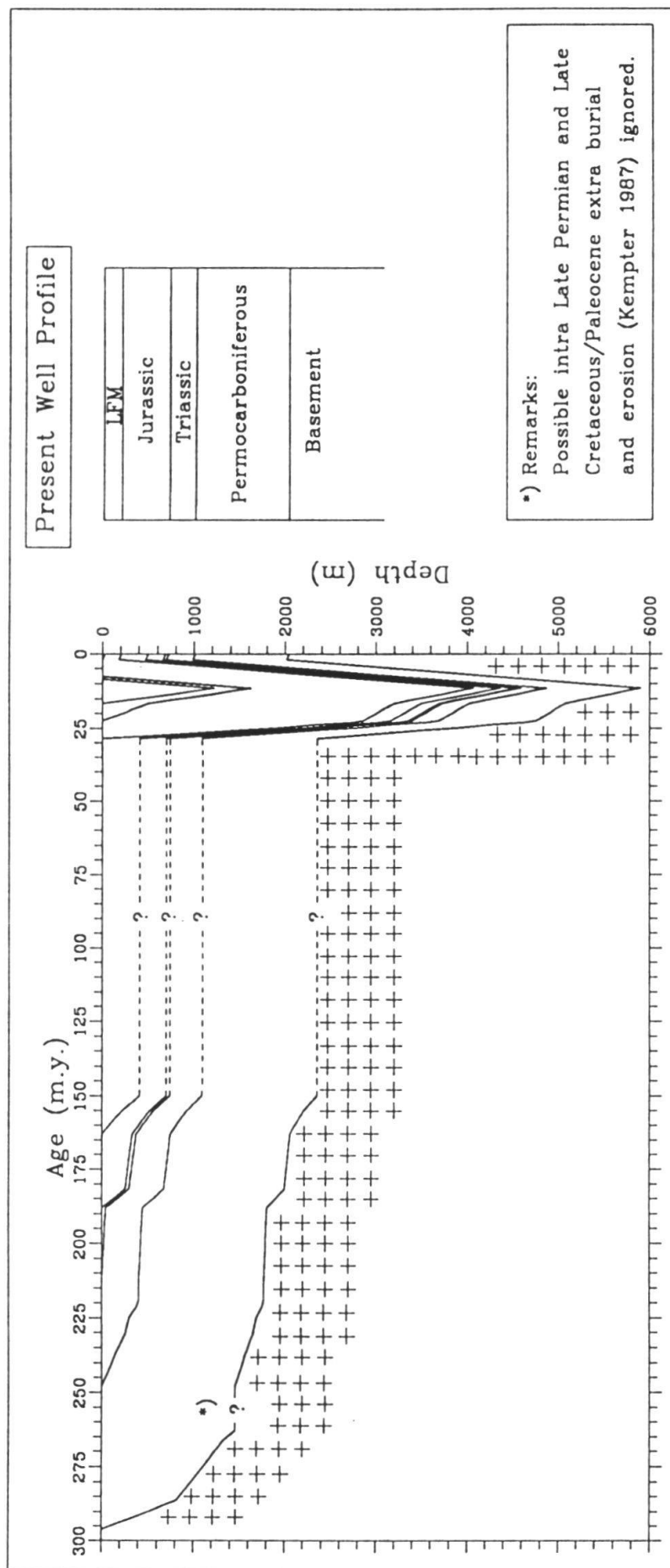
18

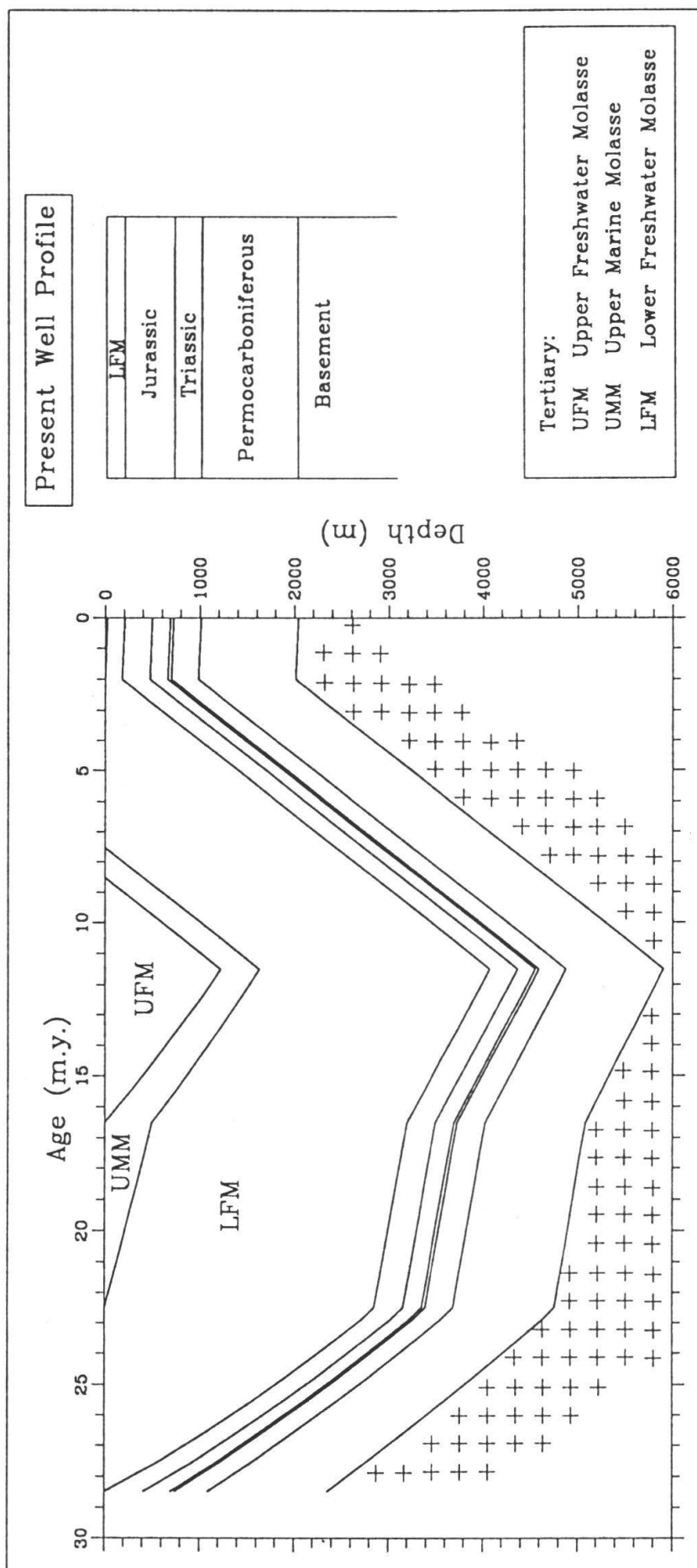**Figure 7** Burial history diagram for the Weiach drillsite.

Figure 8 Burial history diagram for the Weiach drillsite, detailed for the last 30 m.y.
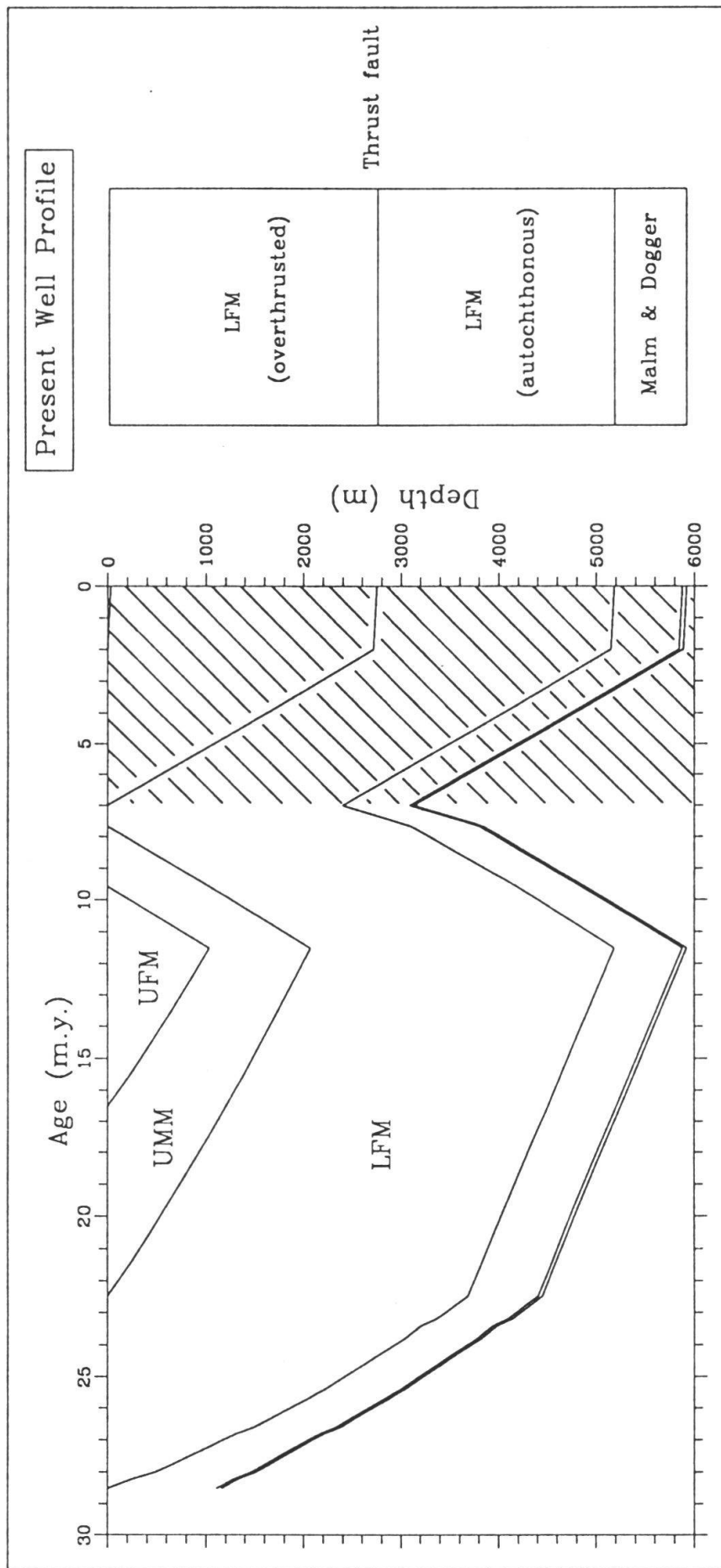
Figure 9 Burial history diagram for the Thun-1 drillsite for the last 30 m.y. Hatchure indicates overthrusting.

Results

Figures 7, 8 and 9 show simplified subsidence curves, taking into account the effect of compaction. Pronounced subsidence and uplift phases can be seen. Figure 7 (Weiach) shows the general subsidence/uplift pattern in the northeast part of the Swiss Molasse basin: Slow and continuous subsidence from Permocarboniferous to Jurassic times; onset of rapid sedimentation/subsidence about 30 m.a. ago, followed by uplift starting about 12 m.a. ago (NAEF et al., 1985). A possible phase of rapid subsidence and uplift/erosion during Late Permian time (KEMPTER, 1987) is ignored at this stage. Figure 8 (Weiach) shows the change of subsidence/uplift rates during the last 30 m.a. In Figure 9 the overthrusting of the Subalpine Molasse units in the southern part of the Swiss Molasse basin is represented similar to a subsidence/sedimentation phase.

From the subsidence/uplift curves the rates of subsidence and uplift as well as their change during the geologic past can be determined. These results are compiled in Table 3.

Table 3   Average Subsidence/Uplift Rates during the Tertiary

Borehole	Age Range (m.y.)	Subsidence Rate (mm/y)	Rates of Uplift (mm/y)
Weiach	28.5 - 22.5	0.60	
	22.5 - 16.5	0.05	
	16.5 - 11.5	0.16	
	11.5 - 2.0		0.41
Schafisheim	28.5 - 22.5	0.52	
	22.5 - 16.5	0.13	
	16.5 - 11.5	0.13	
	11.5 - 2.0		0.48
Thun-1	28.5 - 22.5	0.55	
	22.5 - 16.5	0.13	
	16.5 - 11.5	0.13	
	11.5 - 7.0		0.59
	7.0 - 2.0	0.53	

Conclusions

* According to compaction trends, late to post-Tertiary erosional gaps in the central Swiss Molasse basin range from about 4 km in the north to as much as 8.5 km for the overthrusted Molasse in the south — much larger than expected from previous views based on regional geology.

* The sediments were deposited at rates of 0.1 to 0.6 mm/a.

* Subsequent uplift, starting about 12 m.a. ago, averaged about 0.5 mm/a.

* According to subsidence/uplift diagrams of different sites, the sediments of the northern and southern parts of the Molasse Basin compacted differently: The southern part is characterized by at least two separate major subsidence phases. The younger one is presumably caused by overthrusting of the Subalpine Molasse unit.

* The influence on compaction of lateral tetonic stress and of diagenetic effects in relation to anomalous pore pressures still needs to be investigated.

References

Dresser Atlas (1982) - *Well Logging and Interpretation Techniques.* Dresser Industries, Inc., USA, 228 p.

HEGARTY K.A., WEISSEL J.K., MUTTER J.C. (1988) - *Subsidence History of Australia's Southern Margin: Constraints on Basin Models.* AAPG Bulletin, 72, 615-633.

HOMEWOOD P., ALLEN P.A., WILLIAMS G.D. (1986) - *Dynamics of the Molasse Basin of Western Switzerland.* Spec. Publs Int. Ass. Sediment., 8, 199-217.

HOUSEKNECHT D.W. (1987) - *Assessing the Relative Importance of Compaction Processes and Cementation to Reduction of Porosity in Sandstones.* AAPG Bulletin, 71, 633-642.

ISSLER D.R., BEAUMONT Ch. (1989) - *A Finite Element Model of the Subsidence and Thermal Evolution of the Extensional Basins: Application to the Labrador Continental Margin.* Thermal History of Sedimentary Basins, Springer Verlag, New York, 239-269.

KAELIN B. (1990) - *Gesteinsdichte und Kompaktion im Schweizerischen Molassebecken, abgeleitet aus Bohrlochmessungen.* Diplomarbeit ETH, Zürich, 75 p.

KEMPTER E.H.K. (1987) - *Fossile Maturität, Paläothermogradienten und Schichtlücken in der Bohrung Weiach im Lichte von Modellberechnungen der thermischen Maturität.* Eclogae geol. Helv., 80, 543-552.

MAGARA K. (1978) - *Compaction and Fluid Migration.* Practical Petroleum Geology, Developements in Petroleum Science, 9, Elsevier, Amsterdam, 319 p.

NAEF HCH., DIEBOLD P., SCHLANKE S. (1985) - *Sedimentation und Tektonik im Tertiär in der Nordschweiz.* Technischer Bericht 85-41, NAGRA.

PERRIER R., QUIBLIER J. (1974) - *Thickness Changes in Sedimentary Layers During Compaction History; Methods for Quantitative Evaluation.* AAPG Bulletin, 58, 507-520.

SCHMOKER J.W., HALLEY R.B. (1982) - *Carbonate Porosity Versus Depth: A Predictable Relation for South Florida.* AAPG Bulletin, 66, 2561-2570.

SCHOLLE P.A., HALLEY R.B. (1983) - *Burial Diagenesis in Carbonate Rocks.* AAPG Bulletin, 67, 546.

SCLATER J.G., CHRISTIE P.A.F. (1980) - *Continental Stretching: An Explanation of the Post-Mid-Cretaceous Subsidence of the Central North Sea Basin.* Journal of the Geophysical Research, 85, 3711-3739.

WEBER H.P.., SATTEL G., SPRECHER C. (1986) - *Geophysikalische Daten.* Technischer Bericht 85-50, NAGRA.